

“This document is the Accepted Manuscript version of a Published Work that appeared in final form in Inorganic Chemistry, copyright © American Chemical Society after peer review and technical editing by the publisher. To access the final edited and published work see [insert ACS Articles on Request author- directed link to Published Work, see <http://pubs.acs.org/doi/abs/10.1021/ic501894u>”

Ligand exchange and redox processes in iridium triazolylidene complexes relevant to catalytic water oxidation

Ana Petronilho,[†] Antoni Llobet,^{*,‡} and Martin Albrecht^{*,†}

[†] School of Chemistry & Chemical Biology, University College Dublin, Belfield, Dublin 4, Ireland

[‡] Institute of Chemical Research of Catalonia (ICIQ), Av. Països Catalans 16, 43007 Tarragona, Spain

E-mail: martin.albrecht@ucd.ie, allobet@iciq.cat

Abstract

Iridium(III) complexes containing a bidentate spectator ligand have emerged as powerful catalyst precursors for water oxidation. Here we investigate the initial steps of transformation at the iridium center when using complex $[\text{IrCp}^*(\text{pyr-trz})\text{Cl}]$ **1** (Cp^* = pentamethylcyclopentadienyl, pyr-trz = 4-(2-pyridyl)-1,2,3-triazol-5-ylidene), a potent water oxidation catalyst precursor. Ligand exchange with water is facile and is reversed in the presence of chloride solutions, while MeCN substitution is only effective from the corresponding aqua complex. A $\text{p}K_{\text{a}} = 8.3$ of the aqua complex was determined, which is in agreement with strong electron donation from the triazolydene ligand that is comparable to aryl anions. Evaluation of the pH-dependent oxidation process in aqueous media reveals two regimes, between pH 4–8.5 and above 10.5, where proton-coupled electron transfer processes are occurring. These investigations will help to further optimize water oxidation catalysts and indicate that MeCN as a co-solvent has adverse effects for initiating water coordination in the oxidation process.

Introduction

Artificial photosynthesis through solar water splitting is one of the key technologies currently considered for harvesting and storing transient solar energy.¹⁻⁴ A major hurdle in this endeavor is the highly demanding water oxidation half-cycle, which requires the shuttling of four protons and four electrons to generate O₂.⁵ Over the last few years, iridium complexes have emerged as very powerful catalysts for this water oxidation process.⁶⁻¹⁸ Depending on the ligand design, very high turnover numbers have been achieved.¹⁹

Moreover, kinetic and mechanistic studies have provide increasingly compelling evidence that some complexes are precursors for homogeneous rather than heterogeneous²⁰⁻²² water oxidation catalysts and that the oxidation therefore occurs at an iridium center that is in a well-defined environment.^{19,23-28} This environment has remained elusive up to now despite various efforts to trap and isolate catalytically competent species.²⁹⁻³² In particular iridium cyclopentadienyl complexes [Ir(Cp*)(L,L)X]⁺ containing a chelating *N,N*-, *C,N*-, or *C,C*-bidentate ligand motive afforded high catalytic activity (Cp* = C₅Me₅⁻).^{7-9,17,19,33,34} Post-reaction analyses strongly indicate oxidative degradation of the Cp* ligand^{27,32,33} rather than formation of IrO_x nanoparticles as a heterogeneous catalyst phase. These reactivity pattern underline the relevance of initial steps of transformation at the iridium center as a concept to understand and improve catalytic activity and to reduce the catalyst activation barrier. To this end we have investigated in more detail complex **1** as a representative for the recently discovered highly active water oxidation catalysts comprised of a carbenic spectator ligand bound to an Ir(Cp*) unit (Fig. 1).³ Complex **1** is highly active in cerium(IV)-mediated water oxidation and achieves turnover numbers in excess of 40,000 and thus provides a valuable system for detailing initial ligand substitution and redox processes. In addition, previous work on this complex including detailed kinetic analyses as well as in-situ monitoring of water oxidation by dynamic light scattering and NMR spectroscopy demonstrated that the catalytically active species is well-defined and thus homogeneous rather than less reproducible heterogeneous layer.¹⁹ The studies reported here detail ligand exchange, proton, and electron donor/acceptor behavior of complex **1** and thus shed light on the accessibility of proton-coupled electron transfer processes. These results highlight the relevance of reaction conditions, in particular with respect to added co-solvents.

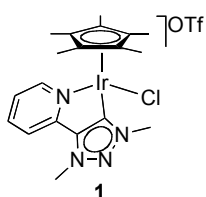


Figure 1 Water oxidation precatalyst iridium complex **1** containing a *N,C*-bidentate pyridyl-triazolylidene ligand.

Results and discussion

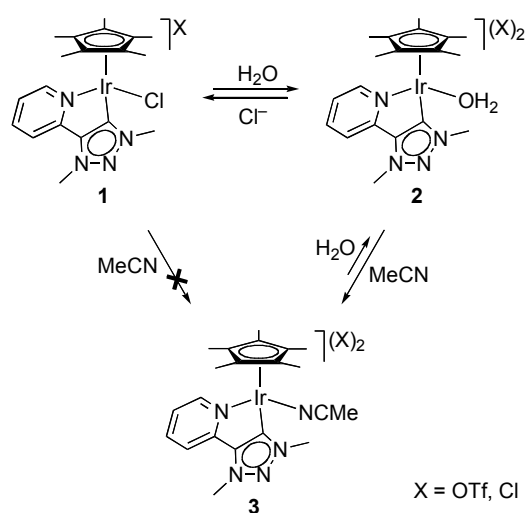
Ligand exchange propensity. Complexes **1–3** were synthesized as the triflate salts according to established procedures.¹⁹ Their behavior in solution was studied in detail. In D₂O, the chloro complex **1** co-exists in a concentration-dependent equilibrium with the dicationic solvento complex **2**, as indicated by the appearance of two sets of pyridine resonances in the ¹H NMR spectrum. The equilibrium is shifted towards **1** in the presence of chloride ions (HCl, NR₄Cl), while addition of HNO₃ (1 M) shifts the equilibrium to the solvento complex **2**. Likewise, **2** is dominant in a 0.1 M aqueous NaOAc solution, and becomes the exclusive species if the NaOAc concentration is raised to 1 M. These results indicate that solvolysis of **1** is promoted by ionic strength, in addition to pH modifications (acid strength). Hydrolysis has also been observed in related anticarcinogenic [Ir(Cp*)Cl(LL)]⁺ complexes under physiological conditions (LL *e.g.* 2,2'-bipyridine).^{35,36}

In contrast to this behavior in water, no chloride dissociation was detected when complex **1** was dissolved in MeCN. Strong chloro coordination to iridium is indicated by the chemical shift of the pyridyl protons in β and γ positions at δ_{H} 8.07 and 8.15 ppm, respectively (*cf* δ_{H} 8.14 and 8.27 ppm for the corresponding solvento complex **3**). The robust Ir–Cl bond of **1** in MeCN is in agreement with the lower polarity of MeCN *vs* H₂O and reflects the low solvation of Cl[–] in MeCN as compared to water. These differences suggest a negative impact of MeCN as a (co-)solvent for catalytic applications because the reduced ionic strength imparted by MeCN will not favor substitution of the chloro ligand.

To probe the coordination strength of MeCN and H₂O to the [Ir(Cp*)(C_{trz}[^]N_{py})]²⁺ unit (C_{trz}[^]N_{py} = 1,3-dimethyl-4-(2-pyridyl)triazol-5-ylidene), the dicationic aqua complex **2** was dissolved in MeCN, and the other way around, the corresponding MeCN complex **3** was dissolved in D₂O. The ¹H NMR spectrum of **2** in CD₃CN features only one set of signals with chemical shifts identical to those of **3** in MeCN, thus indicating complete displacement of the D₂O ligand in **2** by MeCN. Conversely, a solution of the MeCN complex **3** in D₂O reveals two sets of signals due to a mixture of complexes **2** and **3** (2:3 ratio). The two complexes are distinguished most diagnostically by the low field doublet of the pyridyl α proton at δ_{H} 9.10 and 9.01 ppm for **2** and **3**, respectively. The remaining pyridyl protons are magnetically identical in both complexes. Additionally, integration of the resonances for free and coordinated MeCN at 2.38 and 2.06 ppm, corroborates the 2:3 ratio of **2** and **3**. These results reveal that the substitution of MeCN in **3** with water is highly unfavored, and is only partial even in pure water under NMR conditions. Notably, when an aqueous solution of the MeCN

complex **3** is diluted from 10 mM to 1.6 mM, the equilibrium is shifted from the initial 2:3 ratio completely towards **2** (Fig. S1).³⁷

Thus under catalytically relevant conditions (low iridium loading), the aqua complex is the prevailing species when starting from the chloro complex **1** or from the MeCN complex **3**. However, when using MeCN as a (co-)solvent, iridium(III) has a strong preference to bind to this ligand rather than to water and complex **3** becomes the dominant species, with obvious implications for analysis and (catalytic) activity.



Scheme 1 Equilibria of complexes **1**, **2**, and **3** in different solvents.

Determination of pK_a . The pK_a of compound **2** was determined by spectroscopic titration using aqueous solutions buffered at different pHs.^{38,39} Representative UV-vis spectra of the acidic and basic forms are depicted in Fig. 2. The yellow color of the complex solution was persistent and modification of the pH did not result in a visual change of the absorption characteristics. While measurements were run over the entire UV-vis range (200–800 nm), spectroscopic changes only pertained to the UV section of the spectrum (200–400 nm), where complex **2** and its conjugated base showed distinctly different behavior. At pH 6, maxima were observed at 255 and 305 nm (1600 and $1000 \text{ L mol}^{-1} \text{ cm}^{-1}$, respectively) with a shoulder at around 350 nm, while at pH 11, two maximum are located at 280 nm and 340 nm (1400 and $600 \text{ L mol}^{-1} \text{ cm}^{-1}$, respectively). Results from monitoring the pH-dependence of the absorbance at 305 nm are shown in the inset of Fig. 1 (see also Fig. S2, S3).

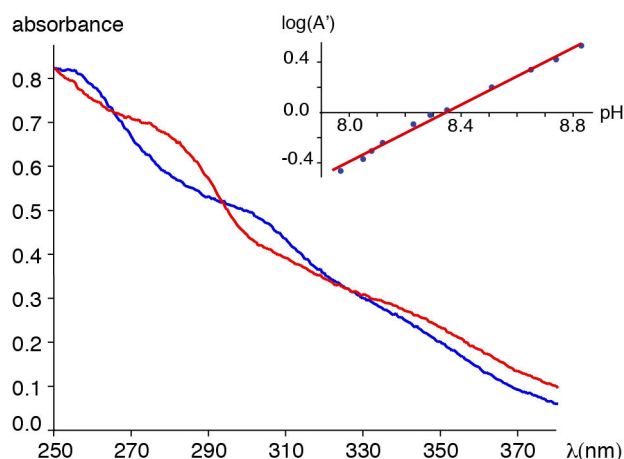


Fig. 2 Representative UV spectra of complex **2** (0.5 mM, in phosphate buffer at 0.1 M ionic strength) at pH 6.3 (blue line) and pH 11.0 (red line); inset: Correlation of pH and the log of the absorbance at $\lambda = 305$ nm for complex **2** with $\log(A') = \log(A - A_{\text{acid}})/(A_{\text{basic}} - A)$.

Deduction of the pK_a from the changes of absorption at 305 and 280 nm was hampered by the relatively small changes in extinction coefficient, hence providing data with limited accuracy ($pK_a = 7.9 \pm 0.2$). Analysis based on the Henderson-Hasselbach equation, *i.e.* by correlating the logarithm of the absorbance vs pH at the wavelengths with diagnostic changes (inset Fig. 2), a slightly higher pK_a was obtained. The data points at $\lambda = 305$ nm afforded a $pK_a = 8.35$, whereas evaluation of the data points at $\lambda = 280$ nm provided a $pK_a = 8.25$. Averaging these values suggests a $pK_a = 8.3 \pm 0.1$ for complex **2** (see also Pourbaix diagram below).

Previous studies indicate that monoaqua complexes $[\text{IrCp}^*(\text{L},\text{L})(\text{H}_2\text{O})]^{2+}$ ($\text{L} = \text{N}$ or O donor ligand) are less acidic than the corresponding tris-aqua complex $[\text{IrCp}^*(\text{H}_2\text{O})_3]^{2+}$.⁴⁰ The pK_a values have also been used to extrapolate the donor ability of the bidentate (L,L) ligand,^{35,36} with a higher pK_a value corresponding to an increased donor capacity of the chelating ligand. The pK_a value obtained for complex **2** supports a stronger donation of the neutral *C,N*-bidentate chelating triazolylidene ligand when compared to neutral *N,O*- or *N,N*-bidentate chelates (*e.g.*, $pK_a \sim 7.2 \pm 0.3$ for $\text{L},\text{L} = 2,2'$ -bipyridine). It is slightly lower than the pK_a of complexes $[\text{IrCp}^*(\text{ppy})(\text{H}_2\text{O})]^{2+}$ containing the anionic and therefore supposedly stronger donating 2-phenylpyridine ligand (pK_a 8.75).³⁵ These values underpin the unique ligand characteristics of mesoionic carbenes as intermediate donors between classically neutral and anionic ligands. We also note that the obtained pK_a value is in excellent agreement with the pK_a deduced from the Pourbaix diagram (see below). A similarly strong influence of the carbene ligand on the electronic properties of a transition metal complex was also noted for related ruthenium complexes.⁴¹

Obviously, the direct correlation of pK_a with donor properties requires caution if the ligand features proton donor/acceptor groups. In such complexes, the pK_a cannot be related exclusively to the donor capacity of a ligand and may be dominated by cooperative hydrogen transfer from coordinated water to such ligands.^{22,34,42} In 1,2,3-triazolylidene complexes, the lone pair at the triazole N(2) site^{43–45} as well as the mesoionic character of the carbene⁴⁶ may potentially be involved in cooperative hydrogen transfer.

Electrochemical analysis. The electrochemical behavior of compounds **1** and **2** was studied by cyclic voltammetry (CV) and differential pulse voltammetry (DPV) in water, CH_2Cl_2 and MeCN. For complex **2**, the measurements were also performed at various pHs and a Pourbaix diagram was constructed from potentials obtained by DPV measurements. No deposition or decomposition of the complexes was detected in any of the measurements, nor an increase in electrocatalytic water oxidation current upon successive scans, which would hint towards the formation of iridium oxide.²¹

In H_2O , complexes **1** and **2** display essentially identical electrochemical behavior, in agreement with the ligand exchange processes described above. A major oxidation wave at +1.21 V is observed at pH 1 (Fig. 3), indicating that chloride oxidation is not interfering with the first oxidation at iridium in **1**. The measurement further underlines that in aqueous acidic solution (*e.g.* aqueous CAN), it is irrelevant whether the chloro complex **1** or its aqua analogue **2** is used as catalyst precursor for water oxidation and both complexes generate the same oxidized species at low pH. The observed oxidation potential is almost 300 mV lower than that reported for analogous complexes with bpy-derived ligands,³⁵ corroborating the stronger donor properties of the triazolylidene compared to pyridine. Complexes **1** and **2** reveal very similar behavior also at higher pH values (Fig. S3). At pH 7, two oxidation curves were identified by DPV. The second oxidation wave is more intense for compound **1**, which may speculatively be due to an overlap with the oxidation of the fraction of complex **1** that has not undergone solvolysis. At pH 11, where complex **2** is almost fully deprotonated and contains hydroxido ligand (ratio hydroxo/aqua 500:1, *cf* pK_a determination above), one major oxidation wave is detected for both complexes at lower potential (+0.84 V). This lower oxidation potential is in agreement with the stronger donor properties of OH^- compared to neutral H_2O .

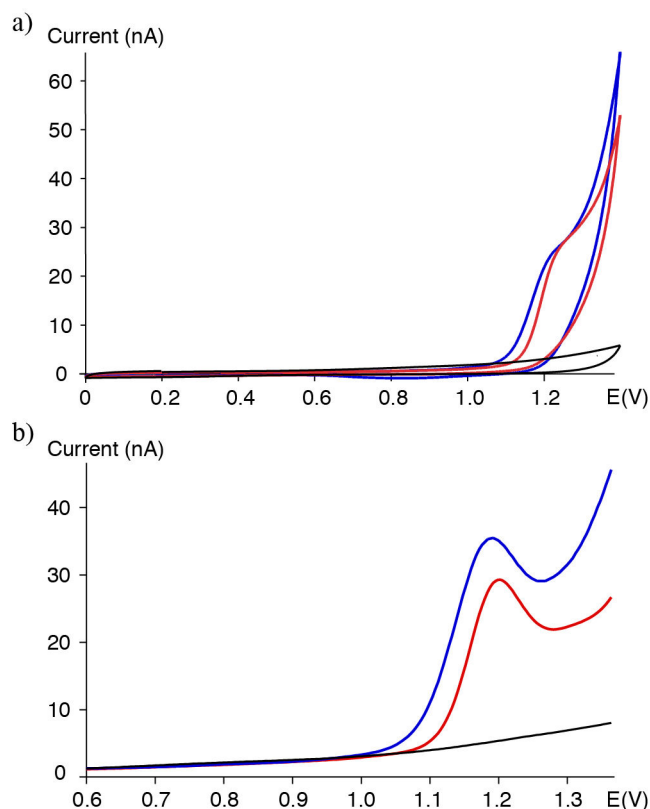


Fig. 3 a) Representative cyclic voltammograms (a) and differential pulse voltammograms (b) for complexes **1** (1.3 mM) and **2** (1.1 mM) at pH 1.1 (0.1 M HNO₃), scan rate 30 mV s⁻¹, E(V) vs SCE.

Due to potential complications imparted by the Cl⁻/H₂O ligand exchange equilibrium with complex **1** upon pH modifications, all further analyses were performed with the aqua complex **2** (X = OTf). This complex was investigated between pH 0 and pH 12.5 at 0.5 pH unit increments to fully map its electrochemical behavior. The CV and DPV experiments were mutually consistent and hence pertinent potentials were extracted from the later. Representative DPV traces at selected pH values are depicted in Fig. 4 and reveal two different oxidation processes,⁴⁷ though the second process is often shallow and not well-resolved (*cf* trace at pH 9.1). This second oxidation wave is only detected in the DPV measurements, suggesting a fast process that is tentatively attributed to a second iridium oxidation. Catalytic solvent oxidation is induced upon further increase of the potential in all measurements.

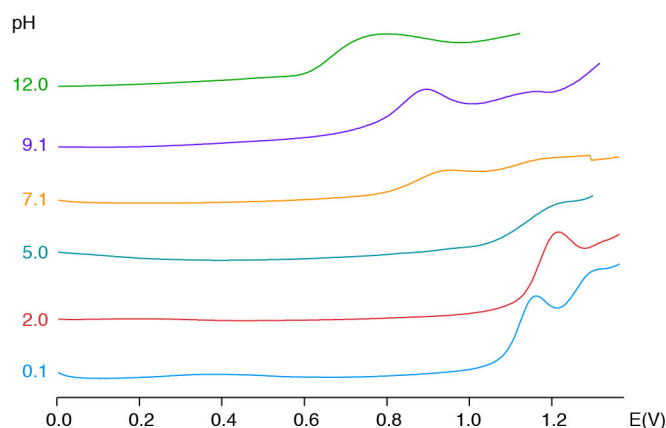


Fig. 4 Differential pulse voltammetry for compound **2** in water at various pHs; E(V) vs SCE, all solutions pH-buffered and at 0.1 M ionic strength (see SI for buffer preparation).

When considering the pH-dependence of the first oxidation process, four specific regions can be distinguished (Fig. 5): below pH 4 and in the pH 8.5–10.5 range, the oxidation process is pH-independent, whereas a pH-dependent oxidation potential is observed in the pH ranges 5.5–8.5, and 10.5–12.5. Accordingly, the constant oxidation potential at low pH suggests an electron transfer that does not involve proton shuttling, *i.e.* oxidation of $\text{Ir}^{\text{III}}\text{--OH}_2$ (**2**) to an $\text{Ir}^{\text{IV}}\text{--OH}_2$ species (**2**⁺). Above pH 4, a pH-dependent electron transfer occurs. The slope of the pH dependence is linear 61(±5) mV/pH (Fig. S4), which is very close to the theoretically predicted 59 mV/pH for a $1\text{H}^+/1\text{e}^-$ process according to the Nernst law.⁴⁸ Hence, a proton-coupled electron transfer (PCET) process is indicated in this regime, involving a net transformation of $\text{Ir}^{\text{III}}\text{--OH}_2$ complex **2** to an $\text{Ir}^{\text{IV}}\text{--OH}$ complex. Further increase of the pH leads again to a pure electron transfer ($\text{Ir}^{\text{III}}\text{--OH}$ to $\text{Ir}^{\text{IV}}\text{--OH}$ in the pH 8.5–10.5 region). At higher pH (pH >10.5), another $1\text{H}^+/1\text{e}^-$ process is revealed by the linear correlation of the oxidation potential and the pH (slope is 63(±5) mV/pH, Fig. S5), yet starting from deprotonated $\text{Ir}^{\text{III}}\text{--OH}$ to produce $\text{Ir}^{\text{IV}}\text{=O}$ by PCET. Such a model is in agreement with an increasing relevance of the hydroxide species upon approaching the $\text{p}K_{\text{a}}$ value.

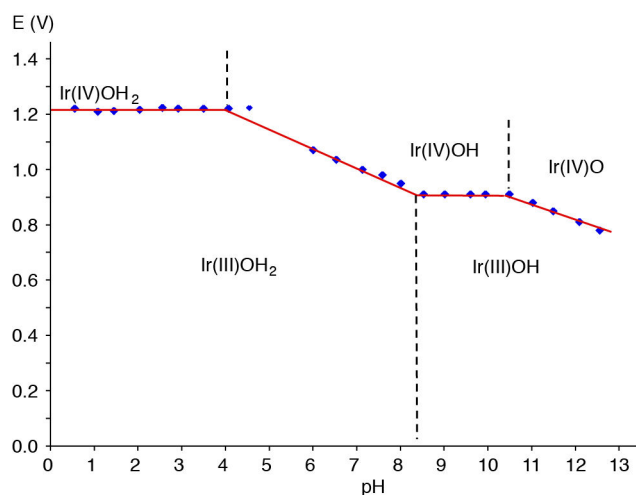


Fig. 5 Pourbaix diagram for complex **2** in water (oxidation potentials from DPV, E(V) vs SCE).

The redox potential of the naturally occurring oxygen evolving complex in photosystem II is known to be leveled due to proton-coupled electron transfer (PCET) processes,^{49,50} which enable consecutive redox processes without the build-up of charge. This effect has been noted with synthetic catalysts based on ruthenium as well⁵¹ and may rationalize the observation of only one oxidation process under basic conditions. The pH-dependence of the oxidation potential of complex **2** and specifically the lower onset potential under basic conditions further supports a PCET to occur also in complex **2**, which may play a critical role in providing an energetically viable catalytic cycle and in enabling high turnover numbers.

Electrochemical measurements of the iridium complex **2** in MeCN disclose significantly different behavior. While the substitution of H₂O as a ligand with MeCN is fast and essentially complete upon dissolution, the monocationic chloro complex **1** is inert towards a similar exchange so that the chloro ligand remains coordinated. This different reactivity of the two complexes **1** and **2** in MeCN is also reflected in their electrochemical properties. Complex **2**, in fact complex **3**, undergoes an irreversible oxidation at high potential (+1.48 V, Fig. 6). In contrast, oxidation of complex **1** occurs already at $E_1 = +1.13$. The lower oxidation potential of complex **1** is in agreement with the stronger donor ability of anionic Cl[−] as compared to a neutral MeCN ligand in **3** and also reflects the slight π -acceptor character of MeCN. The DPV of complex **1** showed a second oxidation at $E_2 = +1.36$ V. A related two-step oxidation has been described for similar iridium chloro complexes,^{17,52} and has been attributed to the intermediate formation of an unstable Ir(IV)-Cl species that decomposes to Ir(III) and Cl₂ gas.²⁹ While the first oxidation potential is similar for complex **1** and related complexes (around +1.1 V), the second potential observed with complex **1** is significantly lower (+1.36 vs +1.6 V) and may thus be associated either with the specific properties of the

triazolylidene ligand, or more likely, with electrocatalytic oxidation of residual water in the MeCN solvent. Support for the latter is provided by the catalytic nature of the measured current. When measured in CH_2Cl_2 , complexes **1** and **2** display almost identical oxidation potentials (+1.47 V and +1.48 V, Fig. S6), indicating that in non-aqueous solutions, proton-coupled electron transfer from the aqua complex occurs at about the same potential as the oxidation of the chloro complex.⁵³ This similarity is obviously a consequence of the tight bonding of the H_2O ligand in CH_2Cl_2 , but not in MeCN.

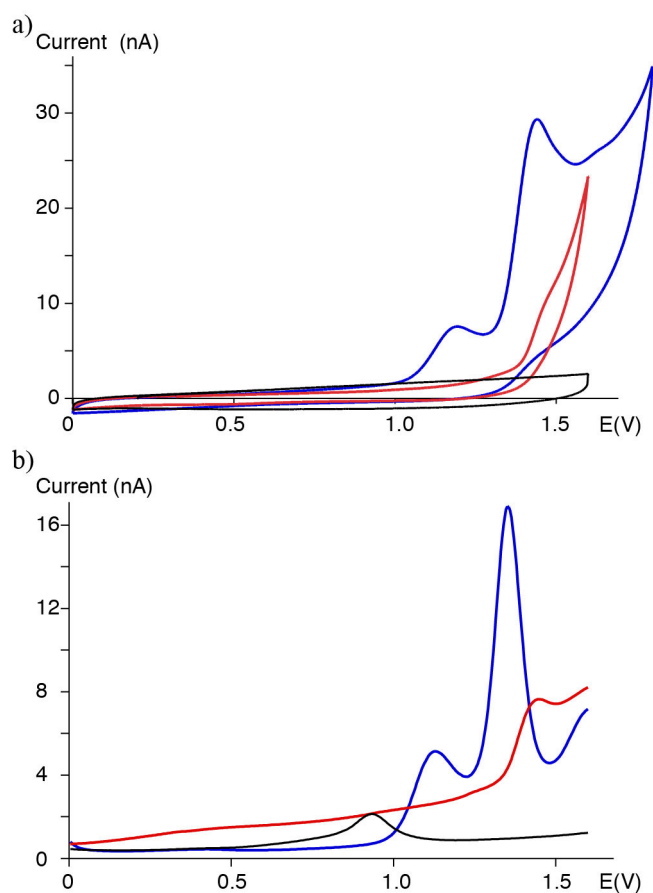


Fig. 6 Representative plots from cyclic voltammetry (a) and differential pulse voltammetry (b) for complexes **1** (1.4 mM, blue curve) and **2** (1.2 mM, red curve) in MeCN; 0.1 M $\text{Bu}_4\text{N}(\text{PF}_6)$ as supporting electrolyte, 30 mVs^{-1} scan rate, E(V) vs SCE.

This work aligns well with previous studies on the pH-dependent oxidation potential of related iridium(III) complexes. For example, an analogue of complex **1** featuring a bpy rather than the pyridyl-carbene as L,L-type ligand was evaluated in the pH 7–12 range and revealed a first oxidation potential which could only be distinguished from the catalytic solvent oxidation at high pH.¹⁰ At pH <7, no oxidation was detected with the bpy analogue, which demonstrates the higher donor ability of the triazolylidene ligand in **1** compared to the

pyridine in the bpy analogue. This easier accommodation of high-valent intermediates may be a key factor for the high catalytic robustness and the high turnover numbers accomplished by complex **1**. The pH-dependence of a carbene-containing iridium(III) complex has also been reported very recently; complex $[\text{Ir}(\text{Cp}^*)(\text{NHC})(\text{OH})]^+$ is formally a penta-coordinate iridium complex (NHC = N,N'-dimethylimidazol-2-ylidene) that forms a dimer with a bis- μ -oxo diiridium core.⁵⁴ Such a process is presumably prevented in **1** because of the rigid chelation of the pyridyl-triazolylidene ligand. Finally, a pH-dependent investigation has also been reported for an iridium(III) bpy complex that was attached to the surface of an ITO electrode via a phosphonate or carboxyl end group bound to the bpy ligand.⁵⁵ Under these conditions the pH-dependent redox-behavior is substantially different from that of **1**, probably due to restricted translational mobility and also because the nature of the second coordination sphere can be radically different in anchored systems. In addition, these anchored complexes lose the molecular homogeneous signature of the precursor complexes, which might suggest the formation of a heterogeneous phase containing IrO_x species. Such simple oxides anchored onto surfaces follow a Nernstian behavior when analyzed at different pH,⁵⁶ in sharp contrast to complex **1** (cf. Fig. 5).

Conclusions

In water, the chloro iridium complex transforms essentially quantitatively to the aqua complex **2** via rapid chloride dissociation, indicating that in aqueous media the (catalytically) active species is identical, irrespective of whether **1** or **2** is used as precursor. Accordingly, the electrochemical behavior in water is identical, irrespective of the starting complex used. The oxidation potential of complex **2** is pH-independent under acidic conditions, yet strongly dependent in neutral and basic media. The slope of the potential vs pH indicates the accessibility of $1\text{H}^+/1\text{e}^-$ processes, in line with a proton-coupled electron transfer process (PCET). While the measured oxidation represents only a first step en route to water oxidation, these insights may provide further guidelines for detailing catalyst activity, especially when using less acidic conditions than those imparted by cerium(IV)-mediated water oxidation.

Significantly, complex **1** displays a distinctly different behavior from that of **2** in MeCN. These observations emphasize the relevance of the conditions used, and indicate that different species can be involved if coordinating solvents other than water are used in water oxidation catalysis, *e.g.* as additives. The use of MeCN therefore substantially increases the complexity of the catalytic system, and relevant active species become even less evident. Our results

indicate that specifically oxidation processes are markedly affected when using such coordinated solvents.

Experimental section

The synthesis of complexes **1–3** was described previously.¹⁹ All electrochemical experiments were performed with a Bio-logic SP-150 potentiostat using a three-electrode cell composed of a glassy carbon disk (3 mm diameter, CH instruments) as working electrode, a platinum disk (2 mm diameter) from CH Instruments as auxiliary electrode, and a Saturated Calomel Electrode (BAS-Japan) as reference electrode. The experiments in MeCN or CH₂Cl₂ contained NBu₄PF₆ (0.1 M) as supporting electrolyte. Measurements in aqueous solutions were performed at different pH as follows: For pH 0–1.5, aqueous HNO₃ solutions (0.1 M) were titrated with NaOH (1 M) to the desired pH; for pH >1.5, aqueous solutions were prepared using different phosphate, acetate, or carbonate buffers at 0.1 M ionic strength and their detailed preparation is included in the supporting information. UV measurements were performed with a Cary 50-UV-Vis Agilent spectrophotometer.

Supporting Information Available: Representative NMR spectra, spectroscopic pK_a determination data, details related to electrochemical measurements and aqueous buffer preparation. This material is available free of charge via the Internet at <http://pubs.acs.org>.

Acknowledgement. We thank Ariana Savini and Carlo Di Giovanni for technical assistance and Johnson-Matthey for a generous loan of iridium. This work was supported financially by Science Foundation Ireland (SRC), European Research Council (PoC-324609, CoG-615653), and MINECO through grant CTQ-2013-49075-R.

References

- (1) Bard, A. J.; Fox, M. A. *Acc. Chem. Res.* **1995**, *28*, 141–145.
- (2) Hammarström, L.; Hammes-Schiffer, S. *Acc. Chem. Res.* **2009**, *42*, 1859–1860 (thematic issue).
- (3) McDaniel, N. D.; Bernhard, S. *Dalton Trans.* **2010**, *39*, 10021–10030.
- (4) Reece, S. Y.; Hamel, J. A.; Sung, K.; Jarvi, T. D.; Esswein, A. J.; Pijpers, J. J. H.; Nocera, D. G. *Science* **2011**, *334*, 645–648.

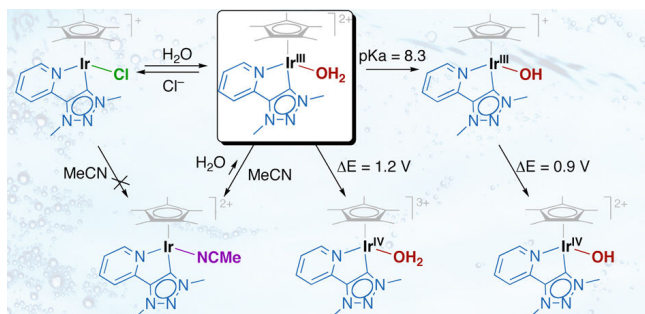
- (5) *Molecular Water Oxidation Catalysis*; Llobet, A., Ed.; Wiley: Chichester (UK), 2014.
- (6) McDaniel, N. D.; Coughlin, F. J.; Tinker, L. L.; Bernhard, S. *J. Am. Chem. Soc.* **2008**, *130*, 210–217.
- (7) Hull, J. F.; Balcells, D.; Blakemore, J. D.; Incarvito, C. D.; Eisenstein, O.; Brudvig, G. W.; Crabtree, R. H. *J. Am. Chem. Soc.* **2009**, *131*, 8730–8731.
- (8) Lalrempuia, R.; McDaniel, N. D.; Müller-Bunz, H.; Bernhard, S.; Albrecht, M. *Angew. Chem., Int. Ed.* **2010**, *49*, 9765–9768.
- (9) Savini, A.; Bellachioma, G.; Ciancaleoni, G.; Zuccaccia, C.; Zuccaccia, D.; Macchioni, A. *Chem. Commun.* **2010**, *46*, 9218–9219.
- (10) Blakemore, J. D.; Schley, N. D.; Balcells, D.; Hull, J. F.; Olack, G. W.; Incarvito, C. D.; Eisenstein, O.; Brudvig, G. W.; Crabtree, R. H. *J. Am. Chem. Soc.* **2010**, *132*, 16017–16029.
- (11) Dzik, W. I.; Calvo, S. E.; Reek, J. N. H.; Lutz, M.; Ciriano, M. A.; Tejel, C.; Hetterscheid, D. G. H.; de Bruin, B. *Organometallics* **2011**, *30*, 372–374.
- (12) Parent, A. R.; Blakemore, J. D.; Brudvig, G. W.; Crabtree, R. H. *Chem. Commun.* **2011**, *47*, 11745–11747.
- (13) Moore, G. F.; Blakemore, J. D.; Milot, R. L.; Hull, J. F.; Song, H. Y.; Cai, L.; Schmuttenmaer, C. A.; Crabtree, R. H.; Brudvig, G. W. *Energy Environ. Sci.*, **2011**, *4*, 2389–2392.
- (14) Parent, A. R.; Brewster, T. P.; Wolf, W. De; Crabtree, R. H.; Brudvig, G. W. *Inorg. Chem.* **2012**, *51*, 6147–6152.
- (15) Petronilho, A.; Rahman, M.; Woods, J. A.; Al-Sayyed, H.; Müller-Bunz, H.; MacElroy, D. J.; Bernhard, S.; Albrecht, M. *Dalton Trans.* **2012**, *41*, 13074–13080.
- (16) Savini, A.; Bellachioma, G.; Bolaño, S.; Rocchigiani, L.; Zuccaccia, C.; Zuccaccia, D.; Macchioni, A., *ChemSusChem* **2012**, *5*, 1415–1419
- (17) Bucci, A.; Savini, A.; Rocchigiani, L.; Zuccaccia, C.; Rizzato, S.; Albinati, A.; Llobet, A.; Macchioni, A. *Organometallics*, **2012**, *31*, 8071–8074.
- (18) Codola, Z.; Cardoso, J. M. S.; Royo, B.; Costas, M.; Lloret-Fillol, J. *Chem. Eur. J.* **2013**, *19*, 7203–7213.
- (19) Woods, J. A.; Lalrempuia, R.; Petronilho, A.; McDaniel, N. D.; Müller-Bunz, H.; Albrecht, M.; Bernhard, S. *Energy Environ. Sci.* **2014**, *7*, 2316–2328.

- (20) Grotjahn, D. B.; Brown, D. B.; Martin, J. K.; Marelus, D. C.; Abadjian, M.-C.; Tran, H. N.; Kalyuzhny, G.; Vecchio, K. S.; Specht, Z. G.; Cortes-Llamas, S. A.; Miranda-Soto, V.; Niekerk, C. van; Moore, C. E.; Rheingold, A. L. *J. Am. Chem. Soc.* **2011**, *133*, 19024–19027.
- (21) Hetterscheid, D. G. H.; Reek, J. N. H. *Chem. Commun.* **2011**, *47*, 2712–2714.
- (22) Hong, D.; Murakami, M.; Yamada, Y.; Fukuzumi, S. *Energy Environ. Sci.* **2012**, *5*, 5708–5716.
- (23) Schley, N. D.; Blakemore, J. D.; Subbaiyan, N. K.; Incarvito, C. D.; D'Souza, F.; Crabtree, R. H.; Brudvig, G. W. *J. Am. Chem. Soc.* **2011**, *133*, 10473–10481.
- (24) Junge, H.; Marquet, N.; Kammer, A.; Denurra, S.; Bauer, M.; Wohlrab, S.; Gärtner, F.; Pohl, M.-M.; Spannenberg, A.; Gladiali, S.; Beller, M. *Chem. Eur. J.* **2012**, *18*, 12749–12758.
- (25) Wang, C.; Wang, J.-L.; Lin, W. *J. Am. Chem. Soc.* **2012**, *134*, 19895–19908.
- (26) deKrafft, K. E.; Wang, C.; Xie, Z.; Su, X.; Hinds, B. J.; Lin, W. *ACS Appl. Mater. Interfaces* **2012**, *4*, 608–613.
- (27) Hintermair, U.; Hashmi, S. M.; Elimelech, M.; Crabtree, R. H. *J. Am. Chem. Soc.* **2012**, *134*, 9785–9795.
- (28) Petronilho, A.; Woods, J. A.; Bernhard, S.; Albrecht, M. *Eur. J. Inorg. Chem.* **2014**, 708–714.
- (29) Brewster, T. P.; Blakemore, J. D.; Schley, N. D.; Incarvito, C. D.; Hazari, N.; Brudvig, G. W.; Crabtree, R. H. *Organometallics* **2011**, *30*, 965–973.
- (30) Zuccaccia, C.; Bellachioma, G.; Bolaño, S.; Rocchigiani, L.; Savini, A.; Macchioni, A. *Eur. J. Inorg. Chem.* **2012**, *2012*, 1462–1468.
- (31) Savini, A.; Belanzoni, P.; Bellachioma, G.; Zuccaccia, C.; Zuccaccia, D.; Macchioni, A. *Green Chem.* **2011**, *13*, 3360–3374.
- (32) Savini, A.; Bucci, A.; Bellachioma, G.; Rocchigiani, L.; Zuccaccia, C.; Llobet, A.; Macchioni, A. *Chem. Eur. J.* **2014**, *20*, 690–697.
- (33) Wang, C.; Xie, Z.; Dekrafft, K. E.; Lin, W. *J. Am. Chem. Soc.* **2011**, *133*, 13445–13454.
- (34) DePasquale, J.; Nieto, I.; Reuther, L. E.; Herbst-Gervasoni, C. J.; Paul, J. J.; Mochalin, V.; Zeller, M.; Thomas, C. M.; Addison, A. W.; Papish, E. T. *Inorg. Chem.* **2013**, *52*,

- 9175–9183.
- (35) Liu, Z.; Habtemariam, A.; Pizarro, A. M.; Fletcher, S. A.; Kisova, A.; Vrana, O.; Salassa, L.; Bruijninx, P. C. A.; Clarkson, G. J.; Brabec, V.; Sadler, P. J. *J. Med. Chem.*, **2011**, 54, 3011–3026.
 - (36) Liu, Z.; Habtemariam, A.; Pizarro, A. M.; Clarkson, G. J.; Sadler, P. J. *Organometallics*, **2011**, 30, 4702–4710.
 - (37) See the supporting information for details.
 - (38) Dadci, L.; Elias, H.; Frey, U.; Hörning, A.; Koelle, U.; Merbach, A. E.; Paulus, H.; Schneider, J. S. *Inorg. Chem.*, **1995**, 34, 306–315.
 - (39) Poth, T.; Paulus, H.; Elias, H.; Dücker-Benfer, C.; van Eldik, R. *Eur. J. Inorg. Chem.*, **2001**, 1361–3169.
 - (40) Two diverging pK_a values were reported for $[\text{IrCp}^*\text{Cl}(\text{bpy})]^+$: 6.86 (from NMR spectroscopy) and 7.5 (from UV-vis spectroscopy), see refs 34 and 35 for details.
 - (41) Masllorens, E.; Rodriguez, M.; Romero, I.; Roglans, A.; Parella, T.; Benet-Buchholz, J.; Poyatos, M.; Llobet, A. *J. Am. Chem. Soc.* **2006**, 128, 5306–5307.
 - (42) Hull, J. F.; Himeda, Y.; Wang, W.; Hashiguchi, B.; Periana, R.; Szalda, D. J.; Muckerman, J. T.; Fujita, E. *Nature Chem.* **2012**, 3, 383–388.
 - (43) Keitz, B. K.; Bouffard, J.; Bertrand, G.; Grubbs, R. H. *J. Am. Chem. Soc.* **2011**, 133, 8498–8501.
 - (44) Tulchinsky, Y.; Iron, M.; Botoshansky, M.; Gandelman, M. *Nat. Chem.* **2011**, 3, 525–531.
 - (45) Tulchinsky, Y.; Kozuch, S.; Saha, P.; Botoshansky, M.; Shimon, L. J. W.; Gandelman, M. *Chem. Sci.* **2014**, 5, 1305–1311.
 - (46) Krüger, A.; Albrecht, M. *Aust. J. Chem.* **2011**, 64, 1113–1117.
 - (47) As pointed out by one of the reviewers, the pH-dependent change of the amplitude of the DPV signals might suggest some more complex behavior than the expected pH effects. However, the Nernstian behavior of the complex points towards the latter.
 - (48) Bard, A. J.; Faulkner, L. R. *Electrochemical Methods: Fundamentals and Applications*; Wiley: Chichester (UK), 2001.
 - (49) Huynh, M. H. V.; Meyer, T. J. *Chem. Rev.* **2007**, 107, 5004–5064.
 - (50) Weinberg, D. R.; Gagliardi, C. J.; Hull, J. F.; Murphy, C. F.; Kent, C. A.; Westlake, B. C.; Paul, A.; Ess, D. H.; McCarty, D. G.; Meyer, T. J. *Chem. Rev.* **2012**, 112, 4016–4093.
 - (51) For an early example, see: Binstead, R. A.; Moyer, B. A.; Samuels, G. J.; Meyer, T. J. *J. Am. Chem. Soc.* **1981**, 103, 2897–2899.

- (52) Brewster, T. P.; Blakemore, J. D.; Schley, N. D.; Incarvito, C. D.; Hazari, N.; Brudvig, G. W.; Crabtree, R. H. *Organometallics*, **2011**, 30, 965–973.
- (53) Francas, L.; Sala, X.; Escudero-Adan, E.; Benet-Buchholz, J.; Escriche, L.; Llobet, A. *Inorg. Chem.* **2011**, 50, 2771–2781.
- (54) Diaz-Morales, O.; Hersbach, T. J. P.; Hetterscheid, D. G. H.; Reek, J. N. H.; Koper, M. T. M. *J. Am. Chem. Soc.* **2014**, 136, 10432–10439.
- (55) Joya, K. S.; Subbaiyan, N. K.; D’Souza, F.; de Groot, H. J. M. *Angew. Chem. Int. Ed.* **2012**, 51, 9601–9605
- (56) Nakagawa, T.; Beasley, C. A.; Murray, R. W. *J. Phys. Chem. C* **2009**, 113, 12958–12961.

For Table of Contents Only



Investigation of the reactivity patterns of a triazolydene iridium aqua complex, which is an excellent water oxidation catalyst precursor, indicates a relatively low pK_a of the metal-bound aqua ligand, a pronounced pH-dependence of the iridium oxidation potential, and selective ligand exchange reactions. Co-solvents such as MeCN have a pronounced and unfavorable impact on the oxidation potential.